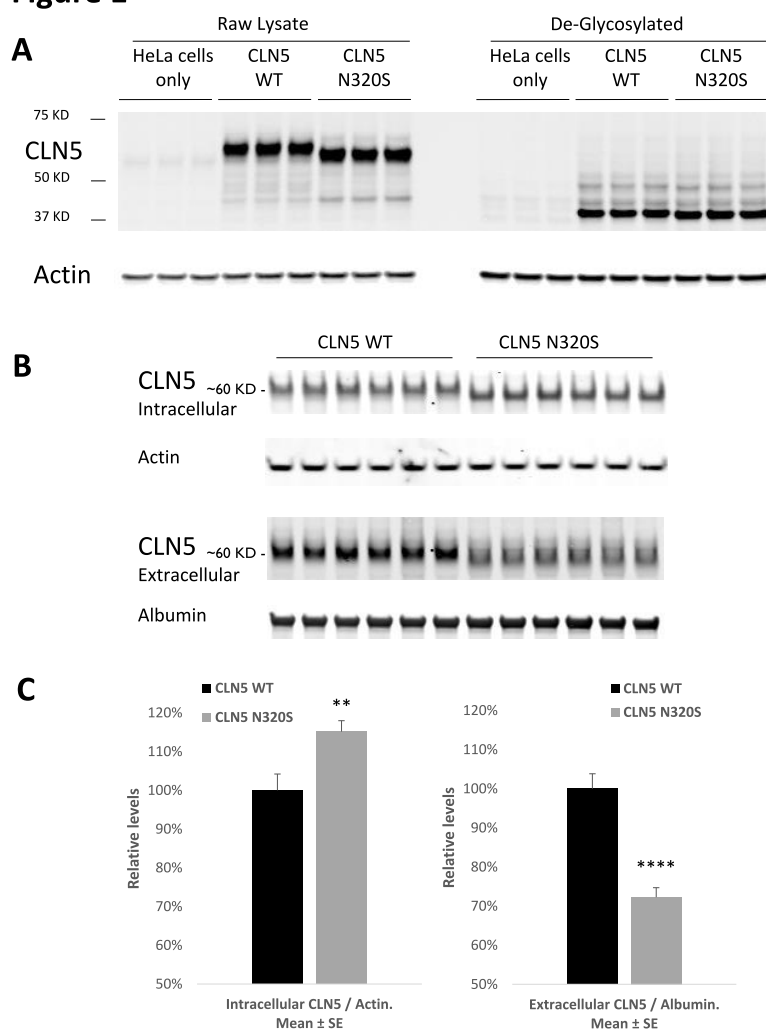
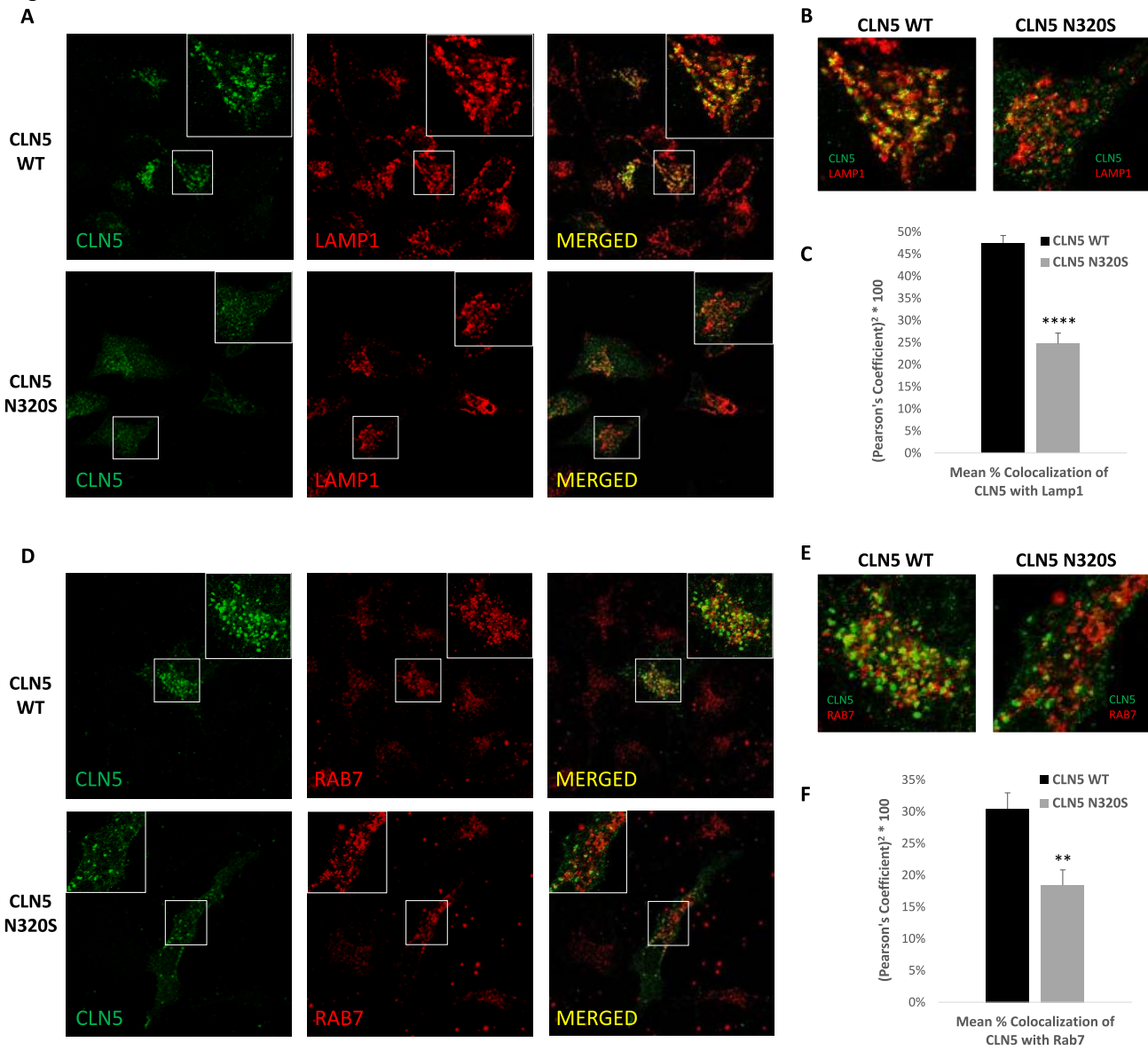


**Figure 1**





**Figure 3**



**Figure 4**

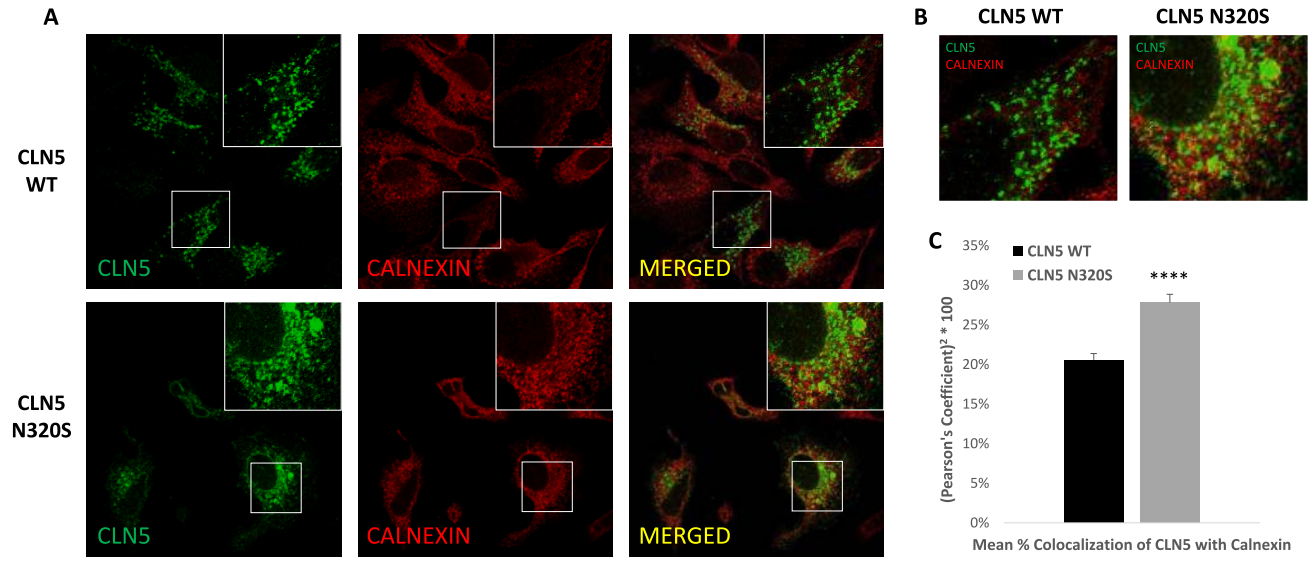


**Figure 5**

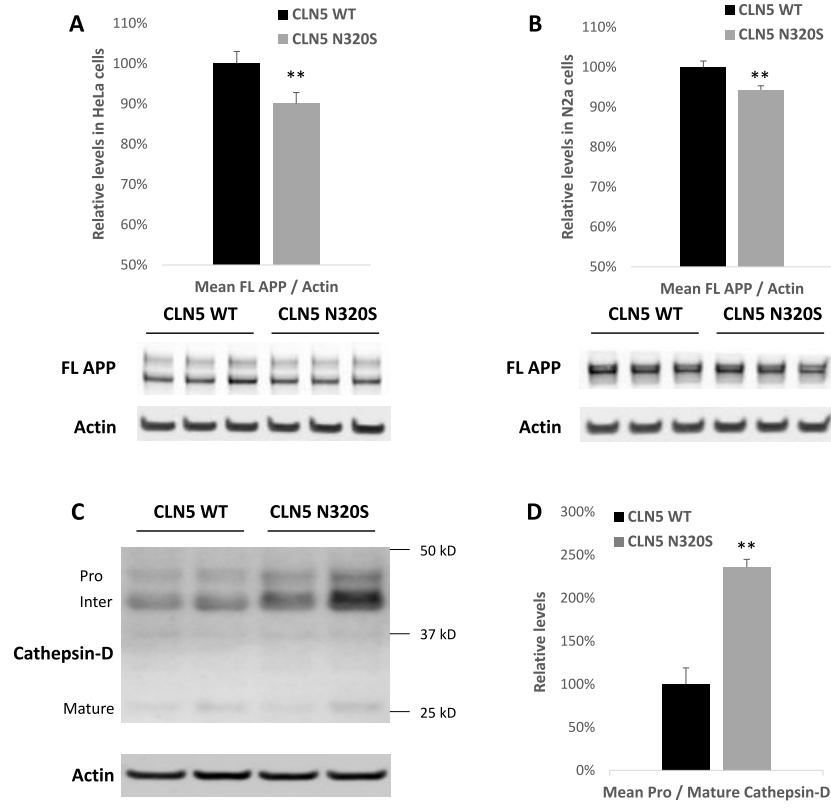
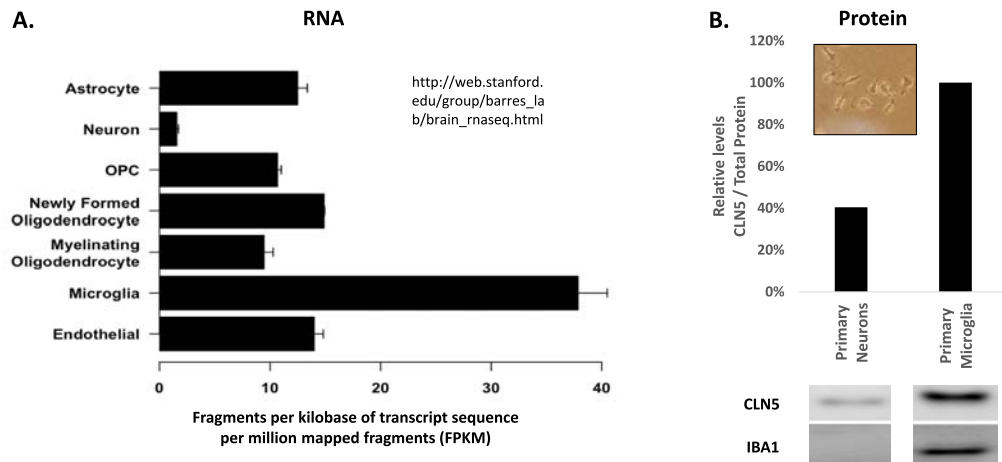


Figure 6





**An Alzheimer's linked loss-of-function CLN5 variant impairs  
Cathepsin D maturation consistent with a retromer trafficking defect**

**Running head:** A *CLN5* variant in Alzheimer's disease

**Authors:** Yasir H Qureshi MD,<sup>1</sup> Vivek M Patel MS,<sup>1</sup> Diego E Berman PhD,<sup>1,5</sup>  
Milankumar J Kothiya MS,<sup>1</sup> Jessica L. Neufeld MA,<sup>1</sup> Badri Vardarajan PhD,<sup>1,2</sup> Min  
Tang PhD,<sup>1,2</sup> Dolly Reyes-Dumeyer BS,<sup>1</sup> Rafael Lantigua MD,<sup>6</sup> Martin Medrano MD,<sup>7</sup>  
Ivonne Jimenez-Velazquez MD,<sup>8</sup> Scott A Small MD,<sup>1,3,5</sup>@ Christiane Reitz MD  
PhD,<sup>1,2,3,4</sup> @

**Affiliations:**

<sup>1</sup>The Taub Institute for Research on Alzheimer's Disease and the Aging Brain,  
Columbia University, New York, NY, USA

<sup>2</sup>The Gertrude H. Sergievsky Center, Columbia University, New York, NY,  
USA <sup>3</sup>Department of Neurology, Columbia University, New York, NY, USA

<sup>4</sup>Department of Epidemiology, Columbia University, New York, NY, USA

<sup>5</sup>Department of Pathology and Cell Biology, Columbia University, New York, NY,  
USA <sup>6</sup>Department of Medicine, Columbia University, New York, NY, USA

<sup>7</sup>School of Medicine, Pontificia Universidad Catolica Madre y  
Maestra, Santiago, Dominican Republic

<sup>8</sup>Department of Internal Medicine, University of Puerto Rico School of  
Medicine, San Juan, Puerto Rico

@correspondence should be addressed to  
[cr2101@cumc.columbia.edu](mailto:cr2101@cumc.columbia.edu) or [sas68@cumc.columbia.edu](mailto:sas68@cumc.columbia.edu)

**Word count**

Title: 16 (127 characters)

Running head: 6 (37 characters)

Abstract: 119

Manuscript Body: 3,057

48  
49  
50  
51  
52  
53**ABSTRACT**

54 In a whole exome sequencing study of multiplex Alzheimer's disease (AD) families we  
55 investigated three neuronal ceroid lipofuscinosis genes that have been linked to retromer,  
56 an intracellular trafficking pathway associated with AD-- Ceroid lipofuscinosis 3 (CLN3),  
57 Ceroid lipofuscinosis 5 (CLN5) and cathepsin D (CTSD). We identified a missense variant  
58 in CLN5 c.A959G (p.Asn320Ser) that segregated with AD. We find that this variant  
59 causes glycosylation defects in the expressed protein, which causes it to be retained in  
60 the endoplasmic reticulum with reduced delivery to the endolysosomal compartment,  
61 CLN5's normal cellular location. The AD-associated CLN5 variant is shown here to  
62 reduce the normal processing of Cathepsin D and to decrease levels of full-length APP,  
63 suggestive of a defect in retromer-dependent trafficking.

64



65 **INTRODUCTION**

66 Lysosomal storage diseases (LSDs) are a group of inherited disorders that typically cause  
67 neurodegeneration early in life(1). Recent observations have established that genetic  
68 variants that cause one type of LSD, Gaucher's disease, can act as a risk factor for  
69 developing a late-onset neurodegenerative disease, Parkinson's disease(2). This  
70 observation suggests that genes that cause other LSDs might act as risk factors for other  
71 late-onset neurodegenerative disorders, notably Alzheimer's disease (AD). While over  
72 the past decade over 25 genes increasing risk of AD have been identified, a large part of  
73 the genetic contribution to AD remains to be clarified (3).

74 With this question in mind, we focused on a select group of genes that cause  
75 another LSD, Neuronal ceroid lipofuscinosis (NCL), because they have been directly or  
76 indirectly associated with retromer trafficking(4, 5). Retromer is a multi-modular protein  
77 assembly that has been linked to the pathogenesis of late-onset AD(6, 7), and is now  
78 considered the 'master conductor' of endosomal sorting and trafficking(8). Among the  
79 group of NCL genes we focused on these three: Ceroid Lipofuscinosis 3 (*CLN3*) whose  
80 expressed protein functions in trafficking the mannose-6-phosphate receptor (M6PR), a  
81 key cargo of retromer(9); *CLN5* whose expressed protein is located at endosomal  
82 membranes and has been shown to function in the recruitment of retromer to endosomal  
83 membranes(4); and CTSD, whose expressed protein, Cathepsin D, requires the normal  
84 retromer-dependent trafficking of M6PR to deliver pro-Cathepsin D to the endosome,  
85 during which it is processed to its mature form Cathepsin D.

86 To explore whether genetic variation in any of these three genes increase risk of  
87 AD, we capitalized on data from a whole exome sequencing study of multiplex  
88 Alzheimer's disease (AD) families. To validate variant(s) identified in these analyses, we  
89 then turned to cell culture to determine whether they have deleterious effects on normal

function. Finally, because all three genes converge on Cathepsin D, we tested whether the abnormal function caused by identified variant(s) would affect the normal processing of this protein.

## MATERIALS AND METHODS

**DNA isolation and sequencing.** High molecular weight DNA was isolated from either fresh or frozen blood stored at  $-80^{\circ}\text{C}$  using the Gentra Puregene and FlexiGene kits (Qiagen). When high quality DNA from blood was unavailable (13 probands), DNA was isolated from lymphocyte cell lines. TruSeq DNA Preparation and Exome Enrichment kits (Illumina, San Diego, CA) were used to prepare indexed genomic DNA (gDNA) libraries and isolate exonic regions for high throughput sequencing. Multiplexed DNA samples were sequenced in batches of up to 12 samples on Illumina's Genome Analyzer IIx, HiSeq 2000, and MiSeq platforms (<http://www.illumina.com>). Paired-end reads were performed over 82-307 sequencing cycles, yielding high coverage at an average depth of  $>60\times$  per sample and interval region captured.

**Downstream bioinformatics analysis of sequence data.** Using the Burrows Wheeler Aligner (10) the reads obtained from the pooled sequencing were aligned to the human reference genome build 37 (<http://bio-bwa.sourceforge.net/>). Quality control of the sequencing data was done using established pipelines, including base alignment quality calibration and refinement of local alignment around putative indels using the Genome Analysis Toolkit (GATK)(11). Variants were called and recalibrated using multi-sample calling with GATK's UnifiedGenotyper and VariantRecalibrator modules. Reliably called variants were annotated by ANNOVAR(12) including *in-silico* functional prediction using POLYPHEN(13) and extent of cross-species conservation using PHYLOP(14).

115 **Statistical analyses of sequence data.** We tested segregation and AD association of  
116 individual single nucleotide variants (SNVs) in the sequenced samples. To validate SNVs  
117 prioritized from these analyses, we genotyped them in all family members of the families  
118 in which they were discovered, and a set of 438 unrelated, unaffected population controls  
119 of similar ancestry (68.1% women, mean age at examination =  $82.0 \pm 7.3$ , *APOE*  $\epsilon 4$  allele  
120 frequency = 9.8%) using the Sequenom MassARRAY platform. We compared their allele  
121 frequencies in affected individuals with unaffected samples from this follow-up genotyping  
122 using Fisher's exact test. The 438 unaffected, unrelated controls were determined to be  
123 of the same ethnic background as the familial cases using methods described  
124 previously(15). We also compared the allele frequencies in affected individuals with the  
125 publicly available ExAC data. Because of the lack of an optimal ethnically matched control  
126 data set for Caribbean Hispanics, we used the ExAC Latino cohort for an estimate of the  
127 population allele frequencies of identified variants.

128 **Design and preparation of the CLN5 constructs.** Plasmids expressing the WT and  
129 c.A959G (N320S) CLN5 proteins (human) tagged with flag at c-terminal were designed  
130 using Thermofisher's GeneArt portal. A flexible poly-glycine linker (6xG) was inserted  
131 between the protein and the tag. mRNA sequence for CLN5 was acquired from the  
132 National Center for Biotechnology Information (NCBI). The constructs were then  
133 subcloned into pcDNA 3.1 (+) Hygro vectors with CMV promotor.

134 **Cell culture.** HeLa cells were cultured using DMEM + 10% FBS and glutamax, with  
135 penicillin, streptomycin and amphotericin B to prevent microbial contamination. Mouse  
136 neuroblastoma (N2a) cells were cultured in 50% DMEM (high glucose) & 50% Opti-MEM  
137 + 10% FBS and Glutamine (2mM) with penicillin and streptomycin to prevent microbial  
138 contamination. Primary mouse cortical neuron cultures were performed as described  
139 previously (16). Primary microglia were cultured as described previously with slight  
140 modifications (17). Briefly brain homogenate from day 1 pups were plated onto poly d

141 ornithine coated flasks in DMEM/F12 + 10% FBS and glutamax containing macrophage  
142 colony stimulating factor (mCSF). At day 7 microglia were dislodged from the bottom of  
143 the flask by tapping the flask gently. Careful tapping results in floating of microglia prior  
144 to other cells / debris. Medium containing microglia was passed through cell strainer to  
145 remove remaining debris. Suspension was spun down at 500g and the pellet was re-  
146 suspended in fresh medium and plated in 6 well plates and allowed to grow and stabilize  
147 for 7 days prior to harvesting.

148 **Transfection of cells with CLN5 WT and N320S variant and biochemistry.** WT and  
149 N320S CLN5 expressing plasmids were transfected into HeLa and N2a cells using  
150 lipofectamine. Cells were harvested 24 hours after transfection, culture medium was also  
151 collected at the same time. Lysates from the samples were run on NuPAGE® Bis-Tris 4-  
152 12% gels, transferred onto nitrocellulose membranes using iblot and were probed with  
153 antibodies against CLN5 (Abcam ab170899 1:500), actin (Novus NB600-535 1:2000),  
154 albumin (abcam ab3781 1:2000), Iba1 (Novus NB100-1028 1:500) Amyloid Precursor  
155 Protein (Abcam ab32136 1:10,000) and cathepsin D (Abcam ab75852 1:500). For the  
156 deglycosylation experiments Endo H kit from New England Biolabs (P0702L) was used  
157 with the recommended protocol ([https://www.neb.com/protocols/2012/10/18/endo-hf-](https://www.neb.com/protocols/2012/10/18/endo-hf-protocol)  
158 [protocol](https://www.neb.com/protocols/2012/10/18/endo-hf-protocol)), briefly lysates were denatured in glycoprotein denaturing buffer at 100°C for 10  
159 min, then incubated in glycobuffer3 and Endo H at 37°C for 1 hour. To generate stable  
160 cell lines some wells of the HeLa cells expressing the CLN5 WT and N320S variant  
161 plasmids were selected with hygromycin B for ~14 days. The surviving stably transfected  
162 cells were plated in 6 well plates, and were harvested after 48 hours for biochemistry.

163 **Immunocytochemistry.** HeLa cells were transfected with CLN5 plasmids in a 24 well  
164 plate (with coverslips) using lipofectamine 2000. Twenty-four hours after transfection cells  
165 were fixed using 4% paraformaldehyde for 10 min and permeabilized using digitonin  
166 (0.01%) for 10 min. To block nonspecific staining cells were incubated in 5% donkey

167 serum overnight. Cells were probed for CLN5 (Abcam ab170899 1:250, Sigma  
168 SAB1412697 1:200), LAMP1 (R&D AF4800 1:500), Rab7 (SC-376362 1:50), and  
169 calnexin (Genescript A01240 1:500) primary antibodies prepared in 1% donkey serum.  
170 Secondary antibodies (Life technologies) conjugated with alexa fluor dyes were used.  
171 Images were taken using Zeiss LSM 700 META confocal microscope equipped with a  
172 63× Plan-Apochromat objective and HeNe1, HeNe2 and argon lasers. Colocalization  
173 analysis was performed using ImageJ's JACoB plugin.

174

## 175 **RESULTS**

### 176 **Whole exome sequencing of multiplex AD families**

177 Whole exome sequencing was performed in 31 Caribbean Hispanic families (98 affected  
178 and 12 unaffected relatives) from the Estudio Familiar de Influencia Genetica en  
179 Alzheimer (EFIGA). Families selected for sequencing had at least four affected individuals  
180 meeting NINCDS-ADRDA(18) standard criteria for AD and were free of known mutations  
181 in *APP*, *PSEN1*, *PSEN2*, *GRN* and *MAPT*. Analysis of the sequence data of the *CLN5*  
182 gene identified a rare missense variant (rs199609750; c.A959G, population frequency:  
183 7.418e-05) that segregated with AD status in one multiplex family, present in two affected  
184 but no unaffected individuals (frequency in affected: 2.0%, frequency in unaffected: 0%).  
185 This variant was also significantly associated with AD when genotyped in all family  
186 members and compared to 438 internally genotyped controls of similar ancestry in which  
187 the mutant allele was entirely absent ( $p < 0.0001$ ), or when compared to population Latino  
188 controls in the ExaC database (allele frequency=0.0006;  $p < 0.0001$ ). No variants in *CLN3*  
189 or *CTSD* were segregating with AD status in these families.

190

### 191 **Altered post-translational processing in the CLN5 c.A959G (N320S) variant**

192 To validate possible biological effects of the CLN5 c.A959G (N320S, rs199609750) AD  
193 variant, we began by expressing WT and c.A959G (N320S) CLN5 in HeLa cells. The WT

194 CLN5 displayed an expected molecular weight of 60kD, however we observed a slight  
195 shift of ~2.5kD in the c.A959G (N320S) variant (**Fig. 1A**). This shift indicates the possibility  
196 of an aberrant post-translational modification, as c.A959G is a missense mutation and  
197 should not result in any form of premature truncation of the protein.

198  
199 CLN5 has 8 asparagine (N) glycosylation sites and all of these sites are  
200 glycosylated in WT human CLN5(19). The c.A959G missense mutation results in the  
201 replacement of the amino acid at position 320, an asparagine with serine (N320S) where  
202 asparagine 320 is one of the glycosylation sites (**Fig. 2**). Moharir et al. (2013) also  
203 indicated that lack of N-glycosylation on certain sites in CLN5, including N320, impairs  
204 CLN5 trafficking and function(19). Based on site-directed mutagenesis of individual  
205 asparagine residues to glutamine on each of the N-glycosylation consensus sites followed  
206 by colocalization studies, they categorized the mutants into three groups: 1. Folding of  
207 the protein without which CLN5 is retained in the ER (N179Q, N252Q, N304Q, N320Q),  
208 2. glycolysation involved in endosome/lysosome trafficking without which CLN5 is  
209 accumulated in the Golgi (N401Q) and 3.) glycolysation involved in lysosomal function  
210 (N192Q, N227Q)), suggesting that there are functional differences in various N-  
211 glycosylation sites of CLN5 which differentially affect folding, trafficking, and lysosomal  
212 function of CLN5. We hypothesized therefore that this novel amino acid substitution  
213 (N320S) should also interfere with N-glycosylation at this particular site. To confirm this  
214 glycosylation deficit, sugar moieties were stripped away from these proteins before  
215 subjecting them to gel electrophoresis. After the deglycosylation reaction both proteins,  
216 the WT and the N320S mutant, resolved at a location close to 37kD and the difference in  
217 molecular weights between them disappeared. We also noticed a 15% increase in the  
218 levels of intracellular CLN5 N320S variant (**Fig. 1B,C**). This increase in levels can be  
219 explained by the glycosylation defect, as it can lead to abnormal folding of CLN5 resulting



220 in endoplasmic reticulum (ER) entrapment (19, 20). If so, and since CLN5 can be secreted  
221 into the extracellular space (19, 21) , ER retention of the CLN5 N320S variant should be  
222 associated with its diminished secretion. Accordingly, we analyzed CLN5 levels in cell  
223 culture medium, and confirming the hypothesis we find a significant decrease in the CLN5  
224 N320S variant released to the media compared to WT CLN5 (**Fig. 1C**). These  
225 experiments establish that the novel AD-linked CLN5 variant is aberrantly glycosylated  
226 and provide biochemical evidence that suggests that the variant might be trapped in the  
227 ER.

228

#### 229 **Impaired cellular localization and retromer-mediated trafficking in the CLN5** 230 **N320S variant**

231 We then turned to confocal microscopy to further confirm this interpretation by comparing  
232 the intracellular localization of WT CLN5 to the AD-associated N320S variant. WT CLN5  
233 is proteolytically cleaved and glycosylated prior to its transport to the endosomal-  
234 lysosomal compartments(21-23). Confirming the hypothesis, compared to WT CLN5, the  
235 AD-associated N320S variant showed increased co-localization with ER markers, but  
236 decreased co-localization with markers of the endosomes and lysosomes (**Fig. 3 and 4;**  
237 **Supplemental Material**).

238 Upon further biochemical analysis of HeLa cells, transiently expressing the WT  
239 and the N320S CLN5, we observed a small but consistent decrease in intracellular full-  
240 length APP (~10% decrease,  $p=0.01$ ), when N320S CLN5 was expressed. To confirm  
241 this finding we repeated these experiments in mouse N2a cells and found a similar  
242 decrease in full-length APP in these neuroblastoma cells (**Fig. 5A-B**).

243 The glycosylation deficiency and ER retention of CLN5 N320S variant suggests  
244 that it is a loss-of-function mutation. One function assigned to CLN5 is its role in retromer  
245 trafficking—a pathway firmly linked to AD etiology by animal, cell biology and genetic



246 studies—based on a study that found that CLN5 depleted cells show evidence of retromer  
247 dysfunction(4). The study relied on previous observations establishing that a reliable  
248 cellular readout of retromer dysfunction is transport defects of Cathepsin D to the  
249 endosomal-lysosomal compartments, a secondary consequence of the dependence of  
250 retromer for mannose-6-phosphate receptor recycling. During the transport to the  
251 endosomal-lysosomal compartments pro-cathepsin D is processed into its mature  
252 form(24), and retromer dysfunction is therefore associated with a relative increase in pro-  
253 cathepsin D compared to mature cathepsin D(25). We relied on this cellular readout to  
254 determine whether the AD-associated CLN5 N320S mutant causes a partial loss of CLN5  
255 function. We measured pro-cathepsin D and mature cathepsin D in HeLa cell lines stably  
256 expressing WT and N320S CLN5 constructs. Compared to cell lines expressing WT  
257 CLN5, we observed a significant increase in pro-cathepsin D levels in the cell lines  
258 expressing CLN5 N320S mutant (**Fig. 5C-D**).

## 259 DISCUSSION

260 Numerous studies focusing on Neuronal Ceroid Lipofuscinosis (NCL) have identified  
261 many NCL related mutations(26). Our findings identify, we believe for the first time, a  
262 variant in one of these genes that is linked to late-onset AD. While CLN5's function is not  
263 fully understood, this transmembrane protein is normally located at endosomal  
264 membranes(19), and one study suggested that it plays a role in retromer trafficking(4).  
265 Retromer is a multi-modular protein assembly that is now considered a 'master  
266 conductor'(8) of endosomal sorting and trafficking. Each retromer module is made up of  
267 a group of proteins that serves a dedicated role, and the modules work together in support  
268 of retromer trafficking function(6). One key module is the 'membrane-recruiting' module,  
269 which functions in recruiting retromer's 'cargo recognition' module to the membrane of  
270 endosomes. The complete list of proteins that are part of the membrane-recruiting  
271 module remains unknown, but a previous study has provided strong evidence that CLN5,

272 which normally resides in the endosome, functions in this module(4). This observation  
273 prompted us to include *CLN5* in our genetic analysis.

274 In a whole exome sequencing study we identified the missense N320S  
275 (p.Asn320Ser) variant in *CLN5* to segregate with AD status in families multiply affected  
276 by the disease. This variant was also significantly associated with AD when genotyped in  
277 all family members and compared to 438 internally genotyped controls of similar ancestry  
278 in which the mutant allele was entirely absent, or when compared to population Latino  
279 controls in the ExaC database. Using a combination of molecular biology, biochemistry,  
280 and immunofluorescence experiments we further validated this variant, functionally  
281 demonstrating that it is glycosylation deficient, which causes the expressed protein to be  
282 partially trapped in the ER and reduces its normal delivery to the endolysosomal system.  
283 Guided by a previous study(4) that showed that *CLN5* deficiency affects retromer's  
284 function, we demonstrate that an effective deficiency in endosomal *CLN5* caused by the  
285 missense variant results in a shift in the relative levels of pro-cathepsin D, an established  
286 phenotype of retromer dysfunction (24, 25, 27, 28), and a reduction in full-length APP.  
287 Genomic and cell biological findings have linked retromer dysfunction to AD  
288 pathogenesis(6). More than simply identifying a *CLN5* variant genetically linked to AD  
289 and validating that it causes a loss-of-function, our results suggest that it converges onto  
290 established pathophysiological mechanisms of disease.

291 We postulate that the identified N320S missense mutant might mediate its AD-  
292 associated toxicity by affecting retromer function in microglia. *CLN5* is highly expressed  
293 in the brain and within the brain *CLN5* is heavily enriched in microglia (**Fig. 6**) (29, 30), a  
294 cell type linked to AD. Microglia are activated upon tissue damage and are critical for  
295 brain homeostasis through clearance of cellular debris. The identification of *CLN5* as a  
296 microglial gene associated with AD is in line with the implication of the microglial gene  
297 *TREM2* (encoding a phagocytic receptor) as an AD susceptibility gene(31). Notably,

298 retromer deficiency has been found in microglia of AD brains(32), but the mechanisms  
299 underlying this deficiency are still unclear. Thus, besides providing additional evidence  
300 for the role and molecular mechanisms of retromer dysfunction in AD, and while the  
301 missense N320S (p.Asn320Ser) variant should be further validated in additional  
302 independent AD datasets and the CLN5 gene should be further scrutinized in various  
303 ethnic groups for additional potential disease-associated variants, our findings provide  
304 critical support for the link between retromer, microglia and AD. Future studies relying on  
305 genetically engineered mice expressing the CLN5 mutation are required to better  
306 establish the functional consequence of this mutation on the brain and its contribution to  
307 various AD-related pathologies, including the potential effect on APP processing  
308 suggested by this study.

309

#### 310 **ACKNOWLEDGEMENTS**

311

312 We would like to thank all participants from the Estudio Familiar de Influencia Genetica  
313 en Alzheimer (EFIGA) for taking part in EFIGA.

314

## 315 REFERENCES

- 316 1. **Plotegher N, Duchen MR.** 2017. Mitochondrial Dysfunction and Neurodegeneration  
317 in Lysosomal Storage Disorders. *Trends Mol Med* **23**:116-134.
- 318 2. **Stirnemann J, Belmatoug N, Camou F, Serratrice C, Froissart R, Caillaud C,**  
319 **Levade T, Astudillo L, Serratrice J, Brassier A, Rose C, Billette de Villemeur T,**  
320 **Berger MG.** 2017. A Review of Gaucher Disease Pathophysiology, Clinical  
321 Presentation and Treatments. *Int J Mol Sci* **18**.
- 322 3. **Lambert JC, Ibrahim-Verbaas CA, Harold D, Naj AC, Sims R, Bellenguez C,**  
323 **DeStafano AL, Bis JC, Beecham GW, Grenier-Boley B, Russo G, Thorton-Wells**  
324 **TA, Jones N, Smith AV, Chouraki V, Thomas C, Ikram MA, Zelenika D,**  
325 **Vardarajan BN, Kamatani Y, Lin CF, Gerrish A, Schmidt H, Kunkle B, Dunstan**  
326 **ML, Ruiz A, Bihoreau MT, Choi SH, Reitz C, Pasquier F, Cruchaga C, Craig D,**  
327 **Amin N, Berr C, Lopez OL, De Jager PL, Deramecourt V, Johnston JA, Evans D,**  
328 **Lovestone S, Letenneur L, Moron FJ, Rubinsztein DC, Eiriksdottir G, Sleegers K,**  
329 **Goate AM, Fievet N, Huentelman MW, Gill M, Brown K, et al.** 2013. Meta-analysis  
330 of 74,046 individuals identifies 11 new susceptibility loci for Alzheimer's disease. *Nat*  
331 *Genet* **45**:1452-1458.
- 332 4. **Mamo A, Jules F, Dumaesq-Doiron K, Costantino S, Lefrancois S.** 2012. The role  
333 of ceroid lipofuscinosis neuronal protein 5 (CLN5) in endosomal sorting. *Mol Cell Biol*  
334 **32**:1855-1866.
- 335 5. **Kama R, Kanneganti V, Ungermann C, Gerst JE.** 2011. The yeast Batten disease  
336 orthologue Btn1 controls endosome-Golgi retrograde transport via SNARE assembly.  
337 *J Cell Biol* **195**:203-215.
- 338 6. **Small SA, Petsko GA.** 2015. Retromer in Alzheimer disease, Parkinson disease and  
339 other neurological disorders. *Nat Rev Neurosci* **16**:126-132.
- 340 7. **Muhammad A, Flores I, Zhang H, Yu R, Staniszewski A, Planel E, Herman M, Ho**  
341 **L, Kreber R, Honig LS, Ganetzky B, Duff K, Arancio O, Small SA.** 2008. Retromer  
342 deficiency observed in Alzheimer's disease causes hippocampal dysfunction,  
343 neurodegeneration, and Abeta accumulation. *Proc Natl Acad Sci U S A* **105**:7327-  
344 7332.
- 345 8. **Burd C, Cullen PJ.** 2014. Retromer: a master conductor of endosome sorting. *Cold*  
346 *Spring Harb Perspect Biol* **6**.
- 347 9. **Metcalf DJ, Calvi AA, Seaman M, Mitchison HM, Cutler DF.** 2008. Loss of the  
348 Batten disease gene CLN3 prevents exit from the TGN of the mannose 6-phosphate  
349 receptor. *Traffic* **9**:1905-1914.
- 350 10. **Li H, Durbin R.** 2009. Fast and accurate short read alignment with Burrows-Wheeler  
351 transform. *Bioinformatics* **25**:1754-1760.
- 352 11. **McKenna A, Hanna M, Banks E, Sivachenko A, Cibulskis K, Kernytsky A,**  
353 **Garimella K, Altshuler D, Gabriel S, Daly M, DePristo MA.** 2010. The Genome  
354 Analysis Toolkit: a MapReduce framework for analyzing next-generation DNA  
355 sequencing data. *Genome Res* **20**:1297-1303.
- 356 12. **Wang K, Li M, Hakonarson H.** 2010. ANNOVAR: functional annotation of genetic  
357 variants from high-throughput sequencing data. *Nucleic Acids Res* **38**:e164.
- 358 13. **Adzhubei IA, Schmidt S, Peshkin L, Ramensky VE, Gerasimova A, Bork P,**  
359 **Kondrashov AS, Sunyaev SR.** 2010. A method and server for predicting damaging  
360 missense mutations. *Nat Methods* **7**:248-249.
- 361 14. **Pollard KS, Hubisz MJ, Rosenbloom KR, Siepel A.** 2010. Detection of nonneutral  
362 substitution rates on mammalian phylogenies. *Genome Res* **20**:110-121.
- 363

15. **Lee JH, Cheng R, Barral S, Reitz C, Medrano M, Lantigua R, Jimenez-Velazquez IZ, Rogaeva E, St George-Hyslop PH, Mayeux R.** 2011. Identification of novel loci for Alzheimer disease and replication of CLU, PICALM, and BIN1 in Caribbean Hispanic individuals. *Arch Neurol* **68**:320-328.
16. **Bhalla A, Vetanovetz CP, Morel E, Chamoun Z, Di Paolo G, Small SA.** 2012. The location and trafficking routes of the neuronal retromer and its role in amyloid precursor protein transport. *Neurobiol Dis* **47**:126-134.
17. **Floden AM, Combs CK.** 2007. Microglia repetitively isolated from in vitro mixed glial cultures retain their initial phenotype. *J Neurosci Methods* **164**:218-224.
18. **McKhann G, Drachman D, Folstein M, Katzman R, Price D, Stadlan EM.** 1984. Clinical diagnosis of Alzheimer's disease: report of the NINCDS-ADRDA Work Group under the auspices of Department of Health and Human Services Task Force on Alzheimer's Disease. *Neurology* **34**:939-944.
19. **Moharir A, Peck SH, Budden T, Lee SY.** 2013. The role of N-glycosylation in folding, trafficking, and functionality of lysosomal protein CLN5. *PLoS One* **8**:e74299.
20. **Lebrun AH, Storch S, Ruschendorf F, Schmiedt ML, Kyttala A, Mole SE, Kitzmuller C, Saar K, Mewasingh LD, Boda V, Kohlschutter A, Ullrich K, Bräulke T, Schulz A.** 2009. Retention of lysosomal protein CLN5 in the endoplasmic reticulum causes neuronal ceroid lipofuscinosis in Asian sibship. *Hum Mutat* **30**:E651-661.
21. **Isosomppi J, Vesa J, Jalanko A, Peltonen L.** 2002. Lysosomal localization of the neuronal ceroid lipofuscinosis CLN5 protein. *Hum Mol Genet* **11**:885-891.
22. **Schmiedt ML, Bessa C, Heine C, Ribeiro MG, Jalanko A, Kyttala A.** 2010. The neuronal ceroid lipofuscinosis protein CLN5: new insights into cellular maturation, transport, and consequences of mutations. *Hum Mutat* **31**:356-365.
23. **Holmberg V, Jalanko A, Isosomppi J, Fabritius AL, Peltonen L, Kopra O.** 2004. The mouse ortholog of the neuronal ceroid lipofuscinosis CLN5 gene encodes a soluble lysosomal glycoprotein expressed in the developing brain. *Neurobiol Dis* **16**:29-40.
24. **Benes P, Vetvicka V, Fusek M.** 2008. Cathepsin D--many functions of one aspartic protease. *Crit Rev Oncol Hematol* **68**:12-28.
25. **Rojas R, van Vlijmen T, Mardones GA, Prabhu Y, Rojas AL, Mohammed S, Heck AJ, Raposo G, van der Sluijs P, Bonifacino JS.** 2008. Regulation of retromer recruitment to endosomes by sequential action of Rab5 and Rab7. *J Cell Biol* **183**:513-526.
26. **Williams RE, Mole SE.** 2012. New nomenclature and classification scheme for the neuronal ceroid lipofuscinoses. *Neurology* **79**:183-191.
27. **Miura E, Hasegawa T, Konno M, Suzuki M, Sugeno N, Fujikake N, Geisler S, Tabuchi M, Oshima R, Kikuchi A, Baba T, Wada K, Nagai Y, Takeda A, Aoki M.** 2014. VPS35 dysfunction impairs lysosomal degradation of alpha-synuclein and exacerbates neurotoxicity in a Drosophila model of Parkinson's disease. *Neurobiol Dis* **71**:1-13.
28. **Follett J, Norwood SJ, Hamilton NA, Mohan M, Kovtun O, Tay S, Zhe Y, Wood SA, Mellick GD, Silburn PA, Collins BM, Bugarcic A, Teasdale RD.** 2014. The Vps35 D620N mutation linked to Parkinson's disease disrupts the cargo sorting function of retromer. *Traffic* **15**:230-244.
29. **Schmiedt ML, Blom T, Blom T, Kopra O, Wong A, von Schantz-Fant C, Ikonen E, Kuronen M, Jauhainen M, Cooper JD, Jalanko A.** 2012. Cln5-deficiency in mice leads to microglial activation, defective myelination and changes in lipid metabolism. *Neurobiol Dis* **46**:19-29.

- 413 30. **Zhang Y, Chen K, Sloan SA, Bennett ML, Scholze AR, O'Keeffe S, Phatnani HP,**  
414 **Guarnieri P, Caneda C, Ruderisch N, Deng S, Liddelow SA, Zhang C, Daneman**  
415 **R, Maniatis T, Barres BA, Wu JQ.** 2014. An RNA-sequencing transcriptome and  
416 splicing database of glia, neurons, and vascular cells of the cerebral cortex. *J*  
417 *Neurosci* **34**:11929-11947.
- 418 31. **Ulland TK, Song WM, Huang SC, Ulrich JD, Sergushichev A, Beatty WL, Loboda**  
419 **AA, Zhou Y, Cairns NJ, Kambal A, Loginicheva E, Gilfillan S, Cella M, Virgin HW,**  
420 **Unanue ER, Wang Y, Artyomov MN, Holtzman DM, Colonna M.** 2017. TREM2  
421 Maintains Microglial Metabolic Fitness in Alzheimer's Disease. *Cell* **170**:649-663 e613.
- 422 32. **Lucin KM, O'Brien CE, Bieri G, Czirr E, Mosher KI, Abbey RJ, Mastroeni DF,**  
423 **Rogers J, Spencer B, Masliah E, Wyss-Coray T.** 2013. Microglial beclin 1 regulates  
424 retromer trafficking and phagocytosis and is impaired in Alzheimer's disease. *Neuron*  
425 **79**:873-886.  
426



## FIGURE LEGENDS

**Fig 1. Glycosylation deficits in AD variant CLN5 N320S.** CLN5 WT and N320S AD variant plasmids were transfected into HeLa cells. After 24 hours the cells were lysed and probed for CLN5. (A) CLN5 migrates to ~60 KD with a difference of approximately 2.5 KD between WT and AD variants, however, when sugar moieties were removed using the enzyme endoglycosidase H, CLN5 resolved to a lower location on the gel at ~37 KD and the molecular weight difference disappeared. (B) The relative level of CLN5 inside the cell was compared to its level in the medium after 24 hours of transfection. WT CLN5 band was observed at ~60KD in both intra & extracellular compartments. (C) Quantification showed a significant increase and decrease in intracellular and extracellular CLN5(N320S) variant respectively. Here and in figures below, asterisks denote \* =  $p < 0.05$ , \*\* =  $p < 0.01$ , \*\*\* =  $p < 0.001$ , and \*\*\*\* =  $p < 0.0001$ .

## Fig 2. Sequence alignment of CLN5 (performed using Clustal Omega

(<http://www.ebi.ac.uk/Tools/msa/clustalo/>)). The red box indicates the N-glycosylation site corresponding to human N320 which is conserved among different species and at which the identified variant rs199609750 (c.A959G) exerts its effect. The green boxes indicate the six additional N-glycosylation sites conserved among different species. The blue boxes indicate the N-glycosylation site corresponding to human N401, which is not conserved in rodents. Sequences used in this alignment: H. sapiens (NP\_006484.1), Bos Taurus (ABD83352.1), Canis lupus familiaris (NP\_001011556.1), Mus musculus (NP\_001028414.1).

**Fig 3. The AD variant CLN5 N320S is reduced in the endolysosomal system.** HeLa cells grown on coverslips were transfected with CLN5 WT and N320S variant plasmids. Cells were fixed with PFA, and stained for CLN5 and LAMP1. (A and B) Co-localization of WT and N320S CLN5 with LAMP1. WT CLN5 staining is more punctate compared to N320S and has a higher colocalization with the lysosomal marker LAMP1. (C) Analysis from 3 independent immunofluorescence experiments showing reduced co-localization of N320S CLN5 with LAMP1 (total no of cells analyzed = 75). (D, E and F) CLN5 co-localization with late endosomal marker RAB7 also followed a pattern similar to LAMP1 colocalization (total no of cells analyzed = 27). For each experiment, the image/cell showing the Pearson correlation value closest to the mean was selected as representative image. \* =  $p < 0.05$ , \*\* =  $p < 0.01$ , \*\*\* =  $p < 0.001$ , and \*\*\*\* =  $p < 0.0001$ .



**Fig 4. Impaired intracellular trafficking in CLN5 N320S cells.** (A and B) Co-localization of WT and N320S CLN5 with ER marker calnexin. (C) Analysis from 3 independent immunofluorescence experiments showing increased co-localization of N320S CLN5 with ER. (total no of cells analyzed = 189). The image/cell showing the Pearson correlation value closest to the mean was selected as representative image. \* =  $p < 0.05$ , \*\* =  $p < 0.01$ , \*\*\* =  $p < 0.001$ , and \*\*\*\* =  $p < 0.0001$ .

**Fig. 5. Reduction of full-length APP and effect on Cathepsin D processing.** HeLa and N2a cells were transfected with CLN5 WT and N320S variant plasmids. After 24 hours, the cells were lysed and probed for full-length APP. (A & B) Full-length APP levels were significantly reduced in CLN5 N320S expressing HeLa and N2a cells. (C) Some wells of the HeLa cells expressing the CLN5 WT and N320S variant plasmids were selected with hygromycin to generate stable cell lines. Stable cell lines were plated in 6 well plates, and after 48 hours the cells were lysed and probed for cathepsin D. (D) Quantification revealed a significant increase in the ratio of pro versus mature cathepsin D. \*\* =  $p < 0.01$ .

**Fig 6. CLN5 Expression in different brain cells.** (A) CLN5 RNA expression measured in Fragments per kilobase of transcript sequence per million mapped fragments (FPKM), reproduced from Ben Barres / Jia Wu database (30) (B) Lysates from primary mouse neurons and primary mouse microglia were probed with anti-CLN5 antibody and anti-IBA1 antibody. Protein levels were normalized to total protein by ponceau stain. (B, inset) Primary microglia at day 7 of culture.